Volume 11
Number 3
21 January 2020
Pages 607-754

Polymer Chemistry

rsc.li/polymers

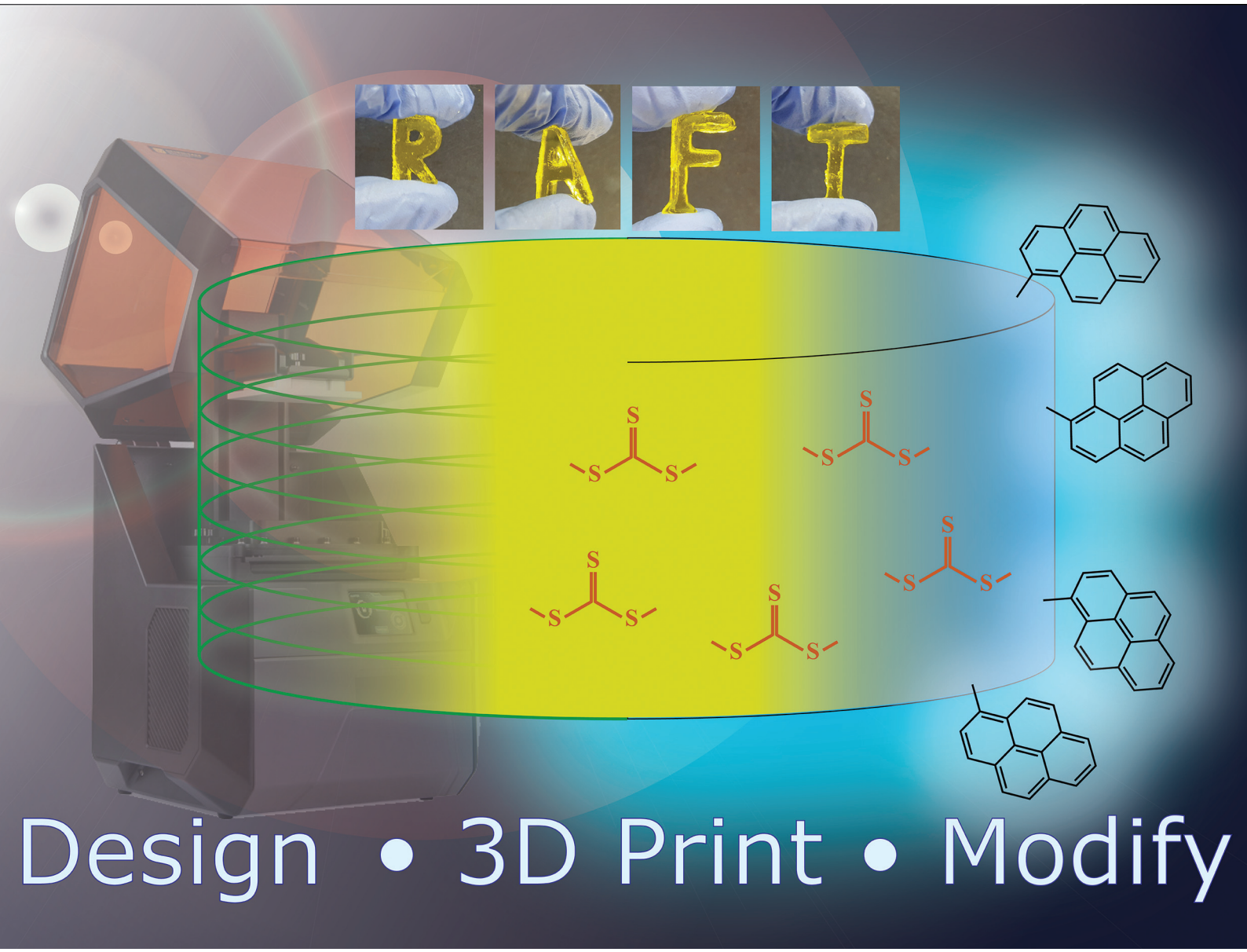

ISSN 1759-9962

ROYAL SOCIETY OF CHEMISTRY

COMMUNICATION
Ali Bagheri, Jianyong Jin *et al.*
3D printing of polymeric materials based on photo-RAFT polymerization

Polymer Chemistry

COMMUNICATION

View Article Online
View Journal | View Issue

Cite this: *Polym. Chem.*, 2020, **11**, 641

Received 20th September 2019,
Accepted 4th November 2019

DOI: 10.1039/c9py01419e

rsc.li/polymers

3D printing of polymeric materials based on photo-RAFT polymerization†

Ali Bagheri, *[a,b] Kyle Edward Engel,[a] Chris William Anderson Bainbridge,[a] Jiangtao Xu,[c] Cyrille Boyer[c] and Jianyong Jin *[a,b]

Here, for the first time, we report the 3D printing of polymeric materials *via* a photo-controlled reversible addition fragmentation chain transfer (photo-RAFT) polymerization process. Our 3D printing resin formulation is based on the use of trithiocarbonate (TTC) RAFT agent, which can mediate radical polymerization *via* direct photolysis under visible light irradiation (λ = 405 nm). Re-activation of the TTC units within the 3D printed materials enables post-printing transformation.

Since the first development of 3D printing technology (otherwise known as additive manufacturing), tremendous effort has been dedicated to further expand its scientific and technological impact in both academic and industrial environments.[1–5] 3D printing techniques have eliminated the need for molds or machining and opened new implementations in various applications such as optical communications, photonics, dentistry, microfluidic and tissue engineering.[6–14] Among various 3D printing methods, photopolymerization-based 3D printing techniques and apparatus such as stereolithography (SLA) and digital light processing (DLP) are currently attracting growing attention due to the versatility of polymer chemistry.[15–19] 3D photopolymerization is mainly based on using nonliving free radical polymerization to cure liquid monomers/oligomers upon exposure to light source of specific wavelength.[20,21] However, the use of conventional free radical polymerization in 3D printing produces "dead" polymers, which prohibits further post-modification.

One possible way to endow cross-linked materials with transformability or "living character" is by introduction of reversible addition fragmentation chain transfer (RAFT)[22–27] agents, such as trithiocarbonates (TTCs), within polymer network.[28–31] TTC species can be re-activated under UV/visible light irradiation, and consequently enable insertion of new monomers into an existing network,[28,31–33] or provide dynamic polymer networks for self-healing or network alterations.[29,32,34–39] For instance, Johnson and co-workers demonstrated UV-induced re-activation of TTC-containing networks for insertion of new monomers into a primary network.[32] It has been demonstrated that specific TTC units can undergo direct photolysis under visible light exposure and act as iniferter units to initiate controlled radical polymerization.[35,40–47] Recently, our group[28] and Matyjaszewski's group in collaboration with Boyer's group[33] have exploited the iniferter properties of TTC units present within photoexpandable/transformable-polymer networks (PET-PNs) to enable post-synthesis modification (*e.g.* monomer insertion) directly under visible light irradiation. Although there have been significant advances in the field of transformable cross-linked networks using TTC species, implementation of these systems in 3D printing have not yet been developed so far.

A broad concept of living additive manufacturing has been initially proposed by Johnson and co-workers in 2017.[31] In their study, a cross-linked network consist of strands bearing TTC iniferters was synthesized (TTC units were embedded in strands of a network *via* coupling of a four-arm polyethylene glycol star polymer terminated with dibenzocyclooctyne and a bis-azide TTC). Blue LED light was used to activate TTC units embedded within polymer networks and thus enable post-synthesis transformations of an initially synthesized gel.[31] Although their approach was efficient in transformation of parent gels into diversely functionalized daughter gels, its application in a practical 3D printing process has not been demonstrated yet.[31,48]

Herein, we report the first example of 3D printing process *via* a photo-RAFT polymerization. Our visible light-curable formulation consists of a TTC iniferter (such as 4-cyano-4-[(dode-

[a]*School of Chemical Sciences, The University of Auckland, Auckland 1010, New Zealand. E-mail: ali.bagheri@auckland.ac.nz, j.jin@auckland.ac.nz*
[b]*Dodd-Walls Centre for Quantum and Photonic Technologies, Auckland 1010, New Zealand*
[c]*Centre for Advanced Macromolecular Design (CAMD) and Australian Centre for NanoMedicine (ACN), School of Chemical Engineering, The University of New South Wales, Sydney NSW 2052, Australia*

† Electronic supplementary information (ESI) available: Chemicals, characterizations and experimental procedures (PDF). See DOI: 10.1039/c9py01419e

cylsulfanylthiocarbonyl) sulfanyl] pentanoic acid (CDTPA)[42–45] or dibenzyl trithiocarbonate (DBTTC)[28]) and a difunctional monomer (such as poly(ethylene glycol) diacrylate (PEGDA 250) or tetra(ethylene glycol) diacrylate (TEGDA)). These solvent-less resin formulations were vigorously deoxygenated and introduced into a modified DLP 3D printer equipped with 405 nm LED lights (1.8 mW cm^{-2}). The photolysis of TTC species under 405 nm light irradiation initiates the photopolymerization of difunctional monomers, and thus, enables layer-by-layer 3D printing process. Parameters of the 3D printing process, such as layer exposure times (8–60 min) and layer thickness (20–100 μm) are pre-defined by a slicing software. Various formulations and printing conditions (printing speed) were evaluated, demonstrating the versatility of our 3D printing process. The resulting 3D printed objects contain the dormant TTC units, which can be re-activated (thermally or under light irradiation) to facilitate post-printing transformation; such as insertion of monomers into an initially 3D printed object. To demonstrate the transformability of the 3D printed materials, monomers of different nature including a fluorescent/light-responsive 1-pyrenemethyl methacrylate (PyMA) monomer and hydrophobic *n*-butyl acrylate (BA) were employed to prepare functional objects with new properties.

Before 3D printing of RAFT-based formulations, we first investigated the photoreactivity of these formulations using photo-differential scanning calorimetry (photo-DSC). Resin formulations with different mole ratios of CDTPA and PEGDA crosslinker were exposed to the photo-DSC light source (the range of wavelength was 315–500 nm) for up to 16 min and the DSC signals were recorded. The effect of CDTPA on the photoreactivity of the RAFT-based formulation was compared to that of formulations containing traditional photoinitiator, such as diphenyl (2,4,6-trimethylbenzoyl) phosphine oxide (TPO). As it can be seen from the Fig. 1a, the non-living TPO-based formulation shows the fastest reaction to reach the maximum of the heat evolution with a t_{max} of 6 s (t_{max} is the time to reach the maximum polymerization rate); which is an indication of the network formation (crosslinking).[49] Replacement of TPO to CDTPA reduces the overall photopolymerization rate of PEGDA and delay the crosslinking process (Fig. 1a). Increasing the content of CDTPA further slows down the photopolymerization reaction. For example, a formulation with a molar ratio of [PEGDA]/[CDTPA] = 1000 : 1 exhibited a t_{max} of ~2.4 min as compared to a [PEGDA]/[CDTPA] = 50 : 1 formulation with a t_{max} of ~10.6 min. This reduction in the photopolymerization reaction rate might be in part due to the slow initiation rate of TTC unites and following chain transfer processes (Fig. 1).[50] It has been previously reported that the exposure of TTC species to visible light results in the excitation of the spin forbidden n → π* transition, leading to β-cleavage of the C–S bond and thereby generation of carbon-centered radicals to initiate polymerization and induce chain transfer (Fig. 1b and c).[28,41,43,45,51–55] It should be noted that this photoiniferter mechanism has been previously reported for preparing linear polymers.[43]

Although the presence of RAFT agents slows down the photopolymerization (photocrosslinking) reaction rate (this is

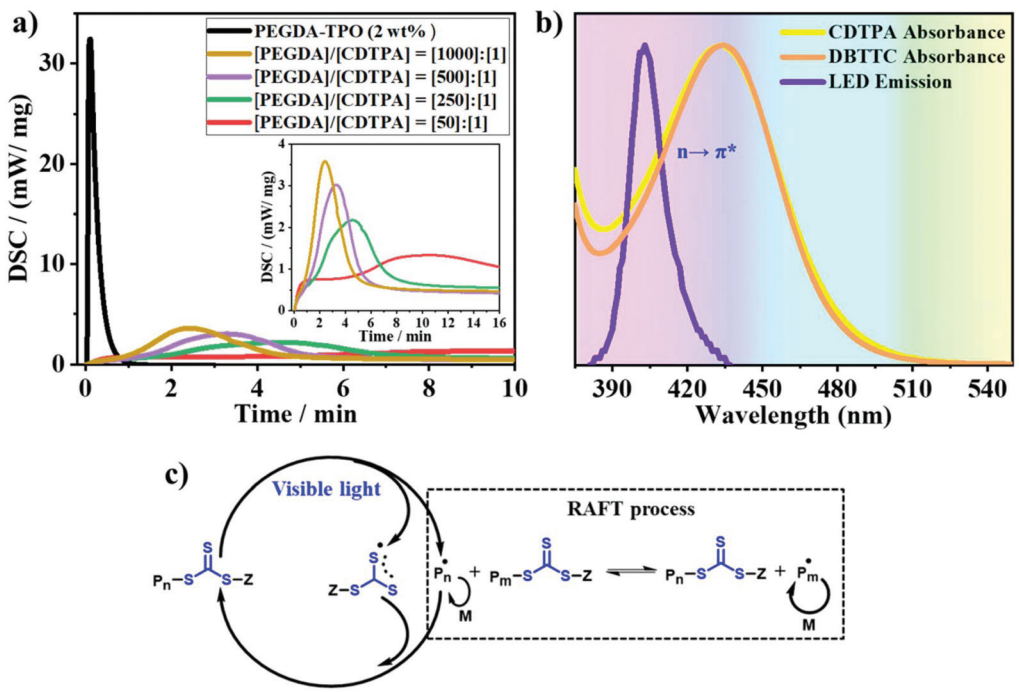

Fig. 1 (a) Photo-DSC plots of different RAFT-based formulations containing CDTPA iniferter, (b) UV-vis absorption spectra of TTC units and the emission spectrum of LED light source of 3D printer, showing emission–absorption overlap (both spectra are normalized) and (c) proposed mechanism of a visible light induced RAFT iniferter approach as previously reported by Qiao's group[56] and Boyer's group.[43]

a compromise to realize RAFT facilitated 3D printing), formulations with high molar ratio of RAFT agents (*e.g.* [PEGDA]/[CDTPA] = 100 : 1 or 50 : 1) were employed for 3D printing processes (Table 1). The reason behind this choice was to produce the 3D printed objects that contain higher content of RAFT agents, which can enable more efficient post-printing monomer insertion *via* re-activation of RAFT agents. This hypothesis originates from our previous report on the post-synthesis transformations of TTC-containing polymer networks.[28]

We then attempted, for the first time, to use these RAFT-based visible light-curable formulations for practical 3D printing process. These formulations were introduced into a modified bottom-up DLP printer where LED lights (λ_{max} = 405 nm, 1.8 mW cm^{-2}) were focused on the bottom surface of the resin vat. The emission spectrum of the LED source of 3D printer was measured, showing clear overlap with CDTPA absorption (Fig. 1b). The 3D fabrication proceeds *via* a layer-by-layer process with pre-defined printing parameters using a slicing software and under a nitrogen atmosphere. The first layer was photopolymerized/cured between the bottom of the vat and the motorized build platform by the LED lights projecting through an in-house built mask for a predefined exposure time (Fig. 2bi and ii). After the formation of the first layer, the build platform moves up in the *z*-direction to lift the printed part from the bottom of the resin vat, which allows the resin to re-flow and fill into the projection area (Fig. 2b-iii). The build platform then moves down in the *z*-direction to create a desired gap at programmed layer thickness between the resin and build platform (Fig. 2b-iv). This layer-by-layer process is repeated until the printing process is completed. It should be noted that our iniferter approach requires no external photocatalyst or initiator to mediate the 3D printing process, which may pose less concerns in the presence of sensitive biological systems (*e.g.*, proteins, cells), and prevents any side products.[45,57]

As the first attempt, a [PEGDA]/[CDTPA] = 100 : 1 was used as the 3D resin (Table 1, entry 1) while the printing parameters were set with an exposure (curing) time of 60 min per layer and layer thickness of 50 μm. These parameters enabled successful 3D printing process as the first demonstration of RAFT-based 3D printing. To further optimize the printing process, lower exposure time of 30 min (Table 1, entry 2) and 15 min (Table 1, entry 3) were also evaluated, which resulted in an increase in the build speed (93 μm h^{-1} for entry 2 and 175 μm h^{-1} for entry 3; Table 1). We also used a mole ratio of [PEGDA]/[CDTPA] = 50 : 1 and printing parameters of 15 min (Table 1, entry 4) and 12 min (Table 1, entry 5) exposure time per 100 μm layer, which resulted in a build speed of 392 μm h^{-1} (Table 1, entry 4) and 485 μm h^{-1} (Table 1, entry 5), respectively. Further reduction in exposure time, *e.g.* 8 min per 100 μm layer (Table 1, entry 6), did not form a 3D structure. This means that under these printing conditions, 100 μm thick layer could not be formed to obtain adequate adhesion to the build platform. By adjusting the layer thickness to 20 μm (while keeping the other parameters constant) the 3D printing process was successful with a build speed of 138 μm h^{-1} (Table 1, entry 7). Optical images of the fabricated 3D structures are presented in Fig. 2c. A scanning electron microscopy (SEM) image of a ~5 mm-tall square (1 cm × 1 cm) comprised of 100 layers (Table 1, entry 2) clearly confirms the stacked layers from a cross sectional view of the printed square (Fig. 2d).

Having demonstrated that a CDTPA iniferter facilitated RAFT-based 3D printing processes, we next studied the use of a different iniferter, such as DBTTC (Fig. 2). Our group previously reported that DBTTC is an effective photoiniferter to fabricate PET-PNs under blue LED (λ_{max} = 460 nm, 0.7 mW cm^{-2}) light irradiation,[28] however, this compound has not been exploited to mediate a 3D printing process yet. A formulation of [PEGDA]/[DBTTC] = 50 : 1 was then prepared and used for 3D printing. Various 3D printing parameters (Table 1, entry 8 to entry 11) were tested, showing a similar trend as CDTPA-based formulations, suggesting that DBTTC iniferter can be also used in a 3D printable RAFT formulation. For example,

Table 1 3D printing using photoiniferter RAFT-based visible light-curable formulations for DLP 3D printing

Entry	[M]/[TTC]	Difunctional oligomers [M]	TTC	Exposure time per layer[a] (min)	Target layer thickness[a] (μm)	Actual build speed[b] (μm h^{-1})
1	100 : 1	PEGDA	CDTPA	60	50	57
2	100 : 1	PEGDA	CDTPA	30	50	93
3	100 : 1	PEGDA	CDTPA	15	50	175
4	50 : 1	PEGDA	CDTPA	15	100	392
5	50 : 1	PEGDA	CDTPA	12	100	485
6	50 : 1	PEGDA	CDTPA	8	100	Failed
7	50 : 1	PEGDA	CDTPA	8	20	138
8	50 : 1	PEGDA	DBTTC	15	100	352
9	50 : 1	PEGDA	DBTTC	12	100	474
10	50 : 1	PEGDA	DBTTC	8	100	Failed
11	50 : 1	PEGDA	DBTTC	8	20	107
12[c]	45(TEGDA) : 5 (BA) : 1	TEGDA BA	DBTTC	30	50	78

[a] Exposure time and target layer thickness are defined by CAD models. [b] The actual build speed is based on the final thickness achieved over time. [c] Entry 12 formulation contained BA monomer. 3D printings were carried out using a modified bottom-up DLP printer equipped with LED lights (λ_{max} = 405 nm, 1.8 mW cm^{-2}) at room temperature and under nitrogen atmosphere.

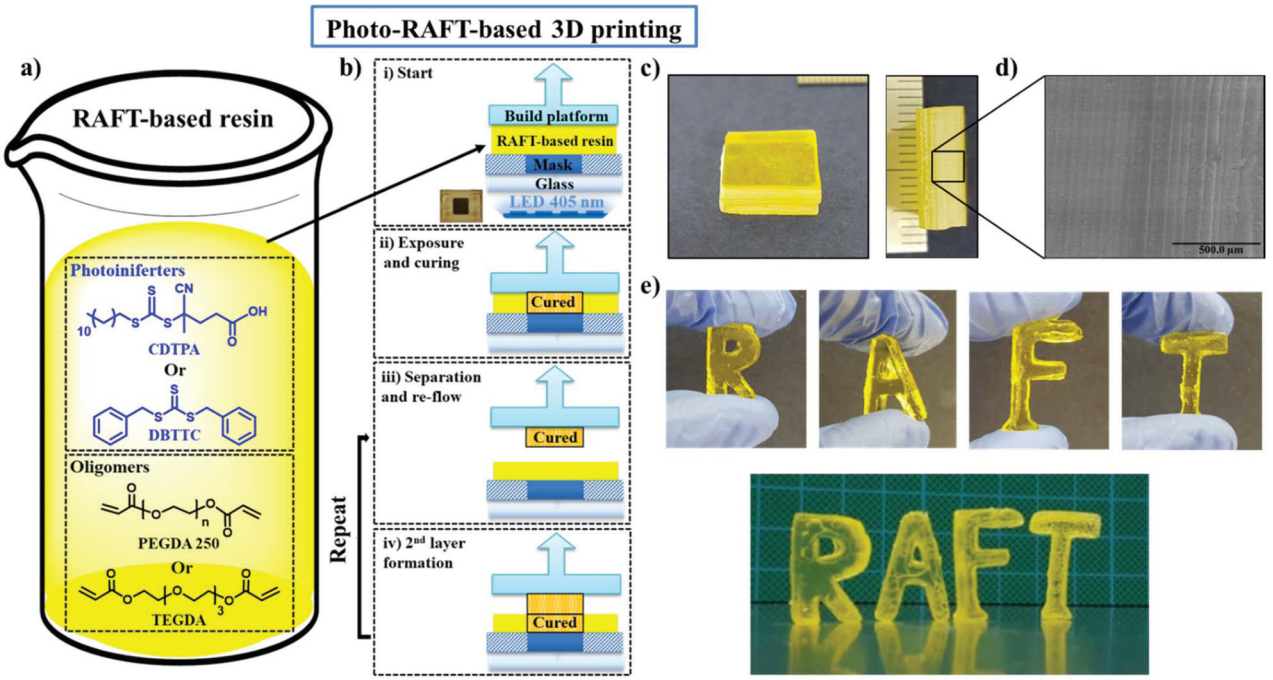

Fig. 2 (a) RAFT-based visible light-curable formulations containing different TTCs: 4-cyano-4-[(dodecylsulfanylthiocarbonyl)sulfanyl]pentanoic acid (CDTPA) and dibenzyl trithiocarbonate (DBTTC); and crosslinkers: poly(ethylene glycol) diacrylate (PEGDA 250) and tetra(ethylene glycol) diacrylate (TEGDA); (b) sequential steps of 3D printing using a modified bottom-up DLP printer equipped with LED lights (λ_{max} = 405 nm, 1.8 mW cm^{-2}) at room temperature and under nitrogen atmosphere; (c) optical image of a 3D square (entry 2); (d) SEM image showing the stacked layers from a cross sectional view of the printed square and (e) optical images of "RAFT" word (entry 9) comprised of 50 layers.

15 min (Table 1, entry 8) and 12 min (Table 1, entry 9) exposure per 100 μm layer resulted in a build speed of 474 μm h^{-1} and 352 μm h^{-1}, respectively. We then adopted the formulation and conditions analogous to entry 9 for 3D printing of the "RAFT" word (Fig. 2e), which comprised of 50 layers.

Further reduction in exposure time to 8 min per 100 μm layer (Table 1, entry 10) was not sufficient to complete a 3D printing process, unless the target layer thickness is reduced to 20 μm (Table 1, entry 11). To further study the scope of this system, we adapted a visible light-curable formulation from our recent study,[28] which consists of a TEGDA as a crosslinker, BA as a co-monomer and a DBTTC photoiniferter ([TEGDA]/[BA]/[DBTTC] = 45 : 5 : 1). Using 30 min exposure per layer (50 μm thickness), 3D materials were printed with a build speed of 78 μm h^{-1} (Table 1, entry 12). This significant reduction in the build speed is due to the addition of a monofunctional BA monomer into the formulation.

Having demonstrated that our RAFT-based formulations can be used in a 3D printing process, we then investigated whether the TTC units present within the 3D printed objects could be re-activated to realize the post-manufacturing modification. Our group[28] and others[33] have previously reported the post-synthesis transformability of TTC-containing networks (network-TTC); however, the examples reported in this contribution are the first demonstrations of post-printing monomer insertion into an initially 3D printed object. To demonstrate this concept, the 3D printed "RAFT" word was adopted as a parent object and subjected to a "growth medium" containing a PyMA monomer and azobisisobutyronitrile (AIBN) thermal initiator. It should be noted that due to the strong absorbance of pyrene monomer in the UV-blue region and possible competition in photo-activation, we selected thermally initiated polymerization for this specific monomer. This post-printing monomer insertion process was performed at 70 °C for 24 h, to afford the pyrene functionalized "RAFT" object (Fig. 3) (see ESI† for details). Fig. 3a shows the image of the modified object (after extensive washing) under 365 nm UV light, exhibiting strong excimer emission of pyrene moieties,[58–64] demonstrating successful insertion of new PPyMA blocks into an initially 3D printed object.

To enable higher accessibility to the TTCs present within the 3D printed object, we printed a thin disc (printing parameters: 15 min exposure time per 100 μm layer; 10 layers; 1 mm total thickness) using a formulation of [PEGDA]/[BA]/[DBTTC] = 45 : 5 : 1. The printed disc was first treated with a PyMA dissolved in DMSO. Polymerization of PyMA, or in another word, PyMA monomer insertion into the printed objects was performed at 70 °C for 24 h. The mass of the dry sample after the monomer insertion (after extensive washing and drying) increased by ~23.9%, demonstrating successful insertion of new PPyMA blocks into an initially printed thin disc. Interestingly, under 365 nm UV light irradiation, the outer layer of the modified disc showed stronger excimer emission of pyrene moieties (visible to the naked eye) as compared

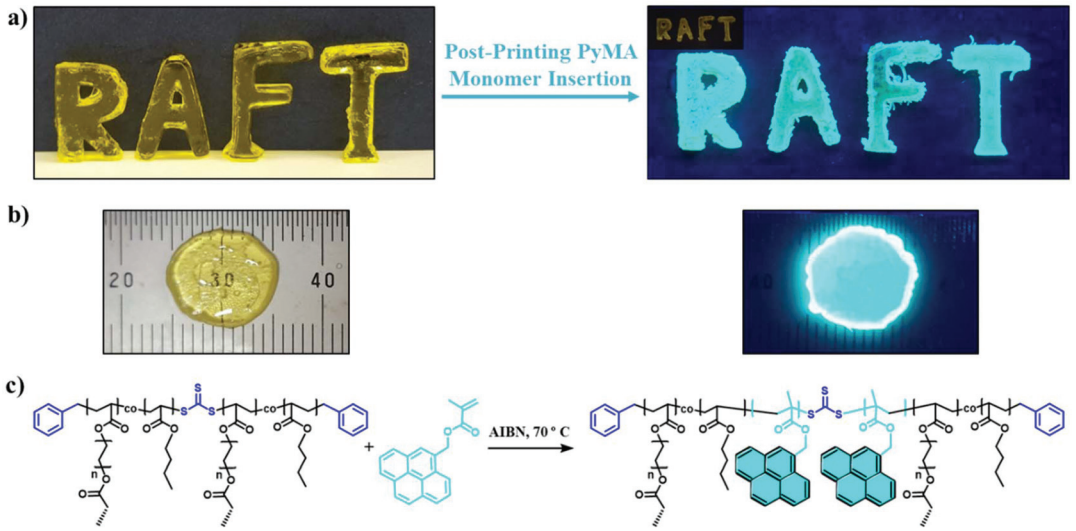

Fig. 3 (a) Optical image of an initially printed "RAFT" word and its subsequent modified network after PyMA insertion; (b) optical image of an initially 3D printed disc and its subsequent modified disc after PyMA insertion (c) reaction scheme of the post-printing PyMA insertion; polymerization of PyMA or in another word, PyMA monomer insertion into the printed objects were performed at 70 °C for 24 h.

to the inner regions of the disc (Fig. 3b).[65,66] This phenomenon shows higher monomer insertion into the regions near the surface where TTCs are more accessible, which is in good agreement with previous reports in the literature.[28,64]

To further prove the versatility of post-printing monomer insertion, we demonstrated the insertion of a hydrophobic BA monomer into a 3D printed sample disc to change its polarity properties. This disc was initially soaked into a growth medium consists of BA monomer dissolved in DMSO, and then exposed to a blue LED light (λ_{max} = 460 nm, 0.7 mW cm^{-2}) to promote photolysis of TTC. To confirm the incorporation of BA monomer into the 3D printed polymer networks, water contact angle measurements were performed to show the change in its hydrophilicity. As it can be seen from Fig. 4, the average contact angle of the modified disc increased from 64.2° to 97.4°, confirming an increase in hydrophobicity of the disc after BA insertion. Collectively, these results demonstrate that 3D printing of TTC-containing materials can be obtained using a RAFT-based formulation. This means new monomers can be inserted into an initially 3D printed objects at the post-printing stage, a characteristic that is not achievable using conventional 3D printing formulations. It should be also noted that due to the high crosslinking density of these 3D printed materials, the second monomer insertions were mostly restricted to the outer layers of the printed object.

In summary, we demonstrate for the first time, the implementation of a photo-RAFT polymerization in a 3D printing process. Our strategy is based on using a visible light-curable formulation containing TTC iniferters that can mediate photopolymerization of cross-linkable monomers and produce

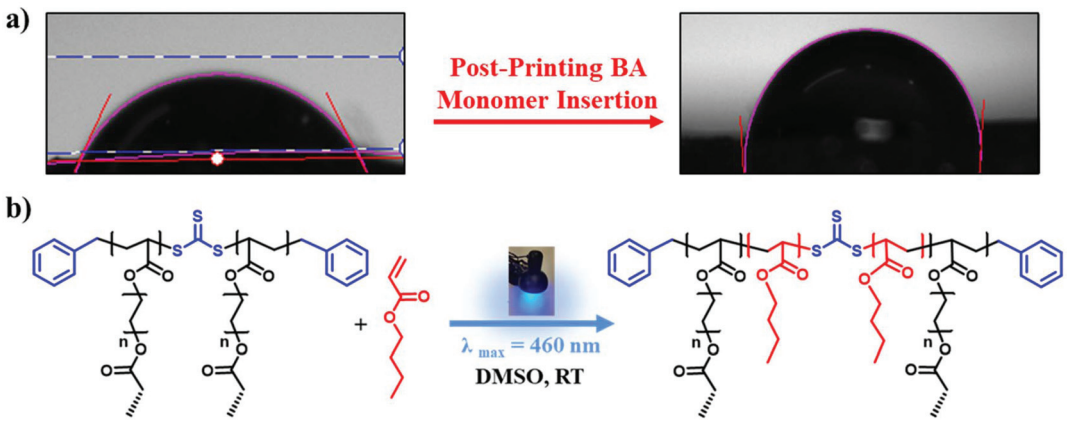

Fig. 4 (a) Water contact angles of an initially printed disc and its subsequent modified network after BA insertion; and (b) reaction scheme of the post-printing BA insertion. Polymerization of BA or in another word, BA monomer insertion into the printed objects was performed under blue LED light (λ_{max} = 460 nm, 0.7 mW cm^{-2}), without presence of external initiators or catalysts.

3D printed materials. Various formulations and printing parameters were evaluated, demonstrating the reproducibility and robustness of our 3D printing approach. Re-activation of the TTC units enables post-printing transformation of 3D printed materials. To demonstrate the versatility of our post-printing modification, monomers of different nature were inserted into initially printed objects to generate progeny materials with chemically distinguished properties. We envisage that our strategy will open up existing 3D printing technologies to a new dimension, which will draw a great deal attention from engineers, material and polymer scientists. Investigations of oxygen tolerant, faster printing speed and extension of viability of RAFT-based systems for the preparation of 3D complex functional materials are currently under investigation in our laboratory[67] and in collaboration with Boyer's research group.[68]

Conflicts of interest

The authors declare no competing financial interest.

Acknowledgements

JJ and AB would like to thank the New Zealand Ministry of Business, Innovation and Employment (MBIE) Endeavour Fund for funding the Advanced Laser Microfabrication for NZ Industries research programme (UOAX-1701).

References

1 A. Bagheri and J. Jin, *ACS Appl. Polym. Mater.*, 2019, **1**, 593–611.
2 S. C. Ligon, R. Liska, J. Stampfl, M. Gurr and R. Mülhaupt, *Chem. Rev.*, 2017, **117**, 10212–10290.
3 M. Layani, X. Wang and S. Magdassi, *Adv. Mater.*, 2018, **30**, 1–7.
4 J. Zhang and P. Xiao, *Polym. Chem.*, 2018, **9**, 1530–1540.
5 A. Al Mousawi, C. Poriel, F. Dumur, J. Toufaily, T. Hamieh, J. P. Fouassier and J. Lalevée, *Macromolecules*, 2017, **50**, 746–753.
6 T. Jungst, W. Smolan, K. Schacht, T. Scheibel and J. Groll, *Chem. Rev.*, 2016, **116**, 1496–1539.
7 M. O. Wang, C. E. Vorwald, M. L. Dreher, E. J. Mott, M. H. Cheng, A. Cinar, H. Mehdizadeh, S. Somo, D. Dean, E. M. Brey and J. P. Fisher, *Adv. Mater.*, 2014, **27**, 138–144.
8 P. Zorlutuna, J. H. Jeong, H. Kong and R. Bashir, *Adv. Funct. Mater.*, 2011, **21**, 3642–3651.
9 E. Shukrun, I. Cooperstein and S. Magdassi, *Adv. Sci.*, 2018, **5**, 1–7.
10 C. Feng, W. Zhang, C. Deng, G. Li, J. Chang, Z. Zhang, X. Jiang and C. Wu, *Adv. Sci.*, 2017, **4**, 1700401.
11 F. Pati, J. Gantelius and H. A. Svahn, *Angew. Chem., Int. Ed.*, 2016, **55**, 4650–4665.
12 K. Seidler, M. Griesser, M. Kury, R. Harikrishna, P. Dorfinger, T. Koch, A. Svirkova, M. Marchetti-Deschmann, J. Stampfl, N. Moszner, C. Gorsche and R. Liska, *Angew. Chem., Int. Ed.*, 2018, **57**, 9165–9169.
13 J. Wang, A. Chiappone, I. Roppolo, F. Shao, E. Fantino, M. Lorusso, D. Rentsch, K. Dietliker, C. F. Pirri and H. Grützmacher, *Angew. Chem., Int. Ed.*, 2018, **57**, 2353–2356.
14 N. Corrigan, J. Yeow, P. Judzewitsch, J. Xu and C. Boyer, *Angew. Chem., Int. Ed.*, 2019, **58**, 5170–5189.
15 M. Zarek, M. Layani, I. Cooperstein, E. Sachyani, D. Cohn and S. Magdassi, *Adv. Mater.*, 2016, **28**, 4449–4454.
16 J. Wang, S. Stanic, A. A. Altun, M. Schwentenwein, K. Dietliker, L. Jin, J. Stampfl, S. Baudis, R. Liska and H. Grützmacher, *Chem. Commun.*, 2018, **54**, 920–923.
17 Y. Guo, Z. Ji, Y. Zhang, X. Wang and F. Zhou, *J. Mater. Chem. A*, 2017, **5**, 16307–16314.
18 Z. Ji, C. Yan, B. Yu, X. Wang and F. Zhou, *Adv. Mater. Interfaces*, 2017, **4**, 1–6.
19 Y. Yang, Z. Chen, X. Song, B. Zhu, T. Hsiai, P. I. Wu, R. Xiong, J. Shi, Y. Chen, Q. Zhou and K. K. Shung, *Nano Energy*, 2016, **22**, 414–421.
20 J. Fu, H. Yin, X. Yu, C. Xie, H. Jiang, Y. Jin and F. Sheng, *Int. J. Pharm.*, 2018, **549**, 370–379.
21 J. Zhang, F. Dumur, P. Xiao, B. Graff, D. Bardelang, D. Gigmes, J. P. Fouassier and J. Lalevée, *Macromolecules*, 2015, **48**, 2054–2063.
22 C. Boyer, V. Bulmus, T. P. Davis, V. Ladmiral, J. Liu and S. Perrier, *Chem. Rev.*, 2009, **109**, 5402–5436.
23 G. Moad, E. Rizzardo and S. H. Thang, *Polymer*, 2008, **49**, 1079–1131.
24 L. Shen, Q. Lu, A. Zhu, X. Lv and Z. An, *ACS Macro Lett.*, 2017, **6**, 625–631.
25 M. R. Hill, R. N. Carmean and B. S. Sumerlin, *Macromolecules*, 2015, **48**, 5459–5469.
26 J. Niu, D. J. Lunn, A. Pusuluri, J. I. Yoo, M. A. O'Malley, S. Mitragotri, H. T. Soh and C. J. Hawker, *Nat. Chem.*, 2017, **9**, 537–545.
27 B. S. Tucker, M. L. Coughlin, C. A. Figg and B. S. Sumerlin, *ACS Macro Lett.*, 2017, **6**, 452–457.
28 A. Bagheri, C. Bainbridge and J. Jin, *ACS Appl. Polym. Mater.*, 2019, **1**, 1896–1904.
29 M. W. Lampley and E. Harth, *ACS Macro Lett.*, 2018, **7**, 745–750.
30 M. Lampley, E. Tsogtgerel and E. M. Harth, *Polym. Chem.*, 2019, **10**, 3799–3924.
31 M. Chen, Y. Gu, A. Singh, M. Zhong, A. M. Jordan, S. Biswas, L. T. J. Korley, A. C. Balazs and J. A. Johnson, *ACS Cent. Sci.*, 2017, **3**, 124–134.
32 H. Zhou and J. A. Johnson, *Angew. Chem., Int. Ed.*, 2013, **52**, 2235–2238.
33 S. Shanmugam, J. Cuthbert, J. Flum, M. Fantin, C. Boyer, T. Kowalewski and K. Matyjaszewski, *Polym. Chem.*, 2019, **10**, 2477–2483.
34 M. B. Gordon, J. M. French, N. J. Wagner and C. J. Kloxin, *Adv. Mater.*, 2015, **27**, 8007–8010.
35 Y. Amamoto, H. Otsuka, A. Takahara and K. Matyjaszewski, *Adv. Mater.*, 2012, **24**, 3975–3980.

36 R. Nicolaÿ, J. Kamada, A. Van Wassen and K. Matyjaszewski, *Macromolecules*, 2010, **43**, 4355–4361.
37 Y. Amamoto, J. Kamada, H. Otsuka, A. Takahara and K. Matyjaszewski, *Angew. Chem., Int. Ed.*, 2011, **50**, 1660–1663.
38 Y. Amamoto, H. Otsuka, A. Takahara and K. Matyjaszewski, *ACS Macro Lett.*, 2012, **1**, 478–481.
39 A. Singh, O. Kuksenok, J. A. Johnson and A. C. Balazs, *Polym. Chem.*, 2016, **7**, 2955–2964.
40 T. G. McKenzie, E. H. H. Wong, Q. Fu, A. Sulistio, D. E. Dunstan and G. G. Qiao, *ACS Macro Lett.*, 2015, **4**, 1012–1016.
41 T. G. McKenzie, Q. Fu, E. H. H. Wong, D. E. Dunstan and G. G. Qiao, *Macromolecules*, 2015, **48**, 3864–3872.
42 J. Yeow, O. R. Sugita and C. Boyer, *ACS Macro Lett.*, 2016, **5**, 558–564.
43 J. Xu, S. Shanmugam, N. A. Corrigan and C. Boyer, in *Controlled Radical Polymerization: Mechanisms*, American Chemical Society, 2015, pp. 247–267.
44 K. Jung, C. Boyer and P. B. Zetterlund, *Polym. Chem.*, 2017, **8**, 3965–3970.
45 A. Bagheri, Z. Sadrearhami, N. N. M. Adnan, C. Boyer and M. Lim, *Polymer*, 2018, **151**, 6–14.
46 X. Pan, G. Jiang, X. Zhu, J. Zhu, C. Fan, Z. Zhang and C. Ding, *Macromol. Rapid Commun.*, 2015, **36**, 2181–2185.
47 T. Otsu, *J. Polym. Sci., Part A: Polym. Chem.*, 2000, **38**, 2121–2136.
48 S. Shanmugam, J. Xu and C. Boyer, *ACS Cent. Sci.*, 2017, **3**, 95–96.
49 C. Gorsche, T. Koch, N. Moszner and R. Liska, *Polym. Chem.*, 2015, **6**, 2038–2047.
50 G. Moad, E. Rizzardo and S. H. Thang, *Aust. J. Chem.*, 2012, **65**, 985–1076.
51 J. R. Lamb, K. P. Qin and J. A. Johnson, *Polym. Chem.*, 2019, **10**, 1585–1590.
52 J. Li, C. Ding, Z. Zhang, X. Pan, N. Li, J. Zhu and X. Zhu, *Macromol. Rapid Commun.*, 2017, **38**, 1–8.
53 Q. Fu, K. Xie, T. G. McKenzie and G. G. Qiao, *Polym. Chem.*, 2017, **8**, 1519–1526.
54 M. A. Tasdelen, Y. Y. Durmaz, B. Karagoz, N. Bicak and Y. Yagci, *J. Polym. Sci., Part A: Polym. Chem.*, 2008, **46**, 3387–3395.
55 S. Dadashi-Silab, S. Doran and Y. Yagci, *Chem. Rev.*, 2016, **116**, 10212–10275.
56 T. G. McKenzie, Q. Fu, E. H. H. Wong, D. E. Dunstan and G. G. Qiao, *Macromolecules*, 2015, **48**, 3864–3872.
57 C. A. Figg, J. D. Hickman, G. M. Scheutz, S. Shanmugam, R. N. Carmean, B. S. Tucker, C. Boyer and B. S. Sumerlin, *Macromolecules*, 2018, **51**, 1370–1376.
58 F. M. Winnik, *Chem. Rev.*, 1993, **93**, 587–614.
59 J. You, J. A. Yoon, J. Kim, C. F. Huang, K. Matyjaszewski and E. Kim, *Chem. Mater.*, 2010, **22**, 4426–4434.
60 S. Nishizawa, Y. Kato and N. Teramae, *J. Am. Chem. Soc.*, 1999, **121**, 9463–9464.
61 Y. Zhao, *Macromolecules*, 2012, **45**, 3647–3657.
62 F. D. Jochum and P. Theato, *Chem. Soc. Rev.*, 2013, **42**, 7468–7483.
63 C. Alvarez-lorenzo, L. Bromberg and A. Concheiro, *Photochem. Photobiol.*, 2009, **85**, 848–860.
64 A. Bagheri, C. Boyer and M. Lim, *Macromol. Rapid Commun.*, 2019, **40**, 1800510.
65 H. Wang, W. Zhang and C. Gao, *Biomacromolecules*, 2015, **16**, 2276–2281.
66 Z. Xu, N. J. Singh, J. Lim, J. Pan, N. K. Ha, S. Park, K. S. Kim and J. Yoon, *J. Am. Chem. Soc.*, 2009, **131**, 15528–15533.
67 A. Bagheri, C. W. A. Bainbridge, K. E. Engel, G. G. Qiao, J. Xu, C. Boyerand J. Jin, *ChemRxiv*, 2019, submitted, DOI: 10.26434/chemrxiv.10116122.
68 Z. Zhang, N. Corrigan, A. Bagheri, J. Jin and C. Boyer, *Angew. Chem., Int. Ed.*, 2019, DOI: 10.1002/anie.201912608.